Article

Xanthine Analogs Suppress *Trypanosoma cruzi* Infection In Vitro Using PDEs as Targets

Amita R. Banga [1,2], Konjeti R. Sekhar [3], Kayla J. Rayford [1], Ashutosh Arun [1], Peace Odiase [1], Amar P. Garg [2], Maria F. Lima [4], Pius N. Nde [1], Fernando Villalta [4,*] and Girish Rachakonda [1,*]

1 Department of Microbiology, Immunology and Physiology, Meharry Medical College, Nashville, TN 37208, USA

2 Department of Biotechnology, School of Biological Engineering & Sciences, Shobhit Institute of Engineering & Technology, Meerut 250110, India

3 Department of Surgical Oncology, Vanderbilt University Medical Center, Nashville, TN 37232, USA

4 Department of Molecular Cellular and Biomedical Sciences, School of Medicine, The City College of New York, New York, NY 10031, USA

* Correspondence: fvillata@med.cuny.edu (F.V.); grachakonda@mmc.edu (G.R.)

Abstract: *Trypanosoma cruzi* (*T. cruzi*), the causative agent of Chagas disease, has infected 6 million people, putting 70 million people at risk worldwide. Presently, very limited drugs are available, and these have severe side effects. Hence, there is an urgency to delve into other pathways and targets for novel drugs. *Trypanosoma cruzi* (*T. cruzi*) expresses a number of different cyclic AMP (cAMP)-specific phosphodiesterases (PDEs). cAMP is one of the key regulators of mammalian cell proliferation and differentiation, and it also plays an important role in *T. cruzi* growth. Very few studies have demonstrated the important role of cyclic nucleotide-specific PDEs in *T. cruzi*'s survival. *T. cruzi* phosphodiesterase C (TcrPDEC) has been proposed as a potential new drug target for treating Chagas disease. In the current study, we screen several analogs of xanthine for potency against trypomastigote and amastigote growth in vitro using three different strains of *T. cruzi* (Tulahuen, Y and CA-1/CL72). One of the potent analogs, GVK14, has been shown to inhibit all three strains of amastigotes in host cells as well as axenic cultures. In conclusion, xanthine analogs that inhibit *T. cruzi* PDE may provide novel alternative therapeutic options for Chagas disease.

Keywords: cAMP; cGMP; phosphodiesterase (PDE); Chagas disease; green fluorescent protein (GFP); *Trypanosoma cruzi* strains; xanthine analogs; IBMX

1. Introduction

Over 1.5 billion people have been infected with various types of neglected tropical diseases, according to the World Health Organization (WHO) [1]. Among them, 6 million people suffer from Chagas disease (CD), with a mortality rate of 12,000 deaths per year [2]. CD is a multisystemic disease that affects the cardiovascular, digestive, and central nervous systems. The causative agent for CD is *Trypanosoma cruzi* (*T. cruzi*), a hemoflagellate protozoan parasite that is transmitted through hematophagous reduviid insects (kissing bugs) in endemic areas such as Latin America [3]. Other routes of transmission include oral and congenital transmission, transfusion, organ transplantation, and laboratory accidents [1]. Globalization and migration have enabled the international spread of the parasite, with 6 million people currently infected and 70 million at risk of infection [1]. As per the U.S. Centers for Disease Control and Prevention (CDC), approximately 300,000 people within the U.S, predominantly immigrants from high-risk areas, are infected, therefore posing a risk to American healthcare [2].

Within the *T. cruzi* lifecycle, the parasite stays in two forms in humans, the trypomastigote form (free circulating form) and the amastigote form (intracellular) [4]. Though

many patients experience few to no symptoms during the acute phase of CD, the intermediate and chronic phases of infection can last for many years. During these phases of CD, intracellular/circulating parasite numbers are reduced; however, the mechanism of pathogenesis remains to be fully understood [5,6]. The majority of infected individuals will continue their life unaffected; however, 30–40% of *T. cruzi*-infected patients will develop cardiovascular, gastrointestinal, and/or neurological disorders [3,7,8].

Despite the discovery of *T. cruzi* a century ago, benznidazole and nifurtimox are presently the only therapeutic options [9,10]. These drugs have limited efficacy and severe adverse effects. Azole inhibitors initially showed prominent results in vitro and in vivo but were ineffective compared to benznidazole in clinical trials [11,12]. The presence of naturally resistant parasite strains further limits their usage and often leads to treatment cessation [10,13]. Thus, there is an urgent need for the development of therapeutics that can efficiently target the many circulating strains.

Cyclic adenosine monophosphate (cAMP), a second messenger, is one of the key regulators in mammalian cell proliferation and differentiation [14]. In the kinetoplastid family of parasites, cAMP plays an important role during cellular invasion and differentiation [15]. Phosphodiesterases (PDEs) are the sole enzymes that hydrolyze cAMP and control cyclic nucleotide signaling in cellular processes [16,17]. In *T. cruzi* kinetoplastids, four families of class I PDEs (A–D) have been identified [18,19], and these enzymes are involved in essential functions, including cell division, osmoregulation, and virulence [20–23]. There is a high level of sequence conservation between mammalian and trypanosomatid PDEs [24]. This is an advantageous tool that can be capitalized on for the treatment of Chagas disease [25], as PDEs are well-known pharmacological targets for various diseases in humans [16,26,27].

IBMX (3-isobutyl-1-methylxanthine) is a non-specific phosphodiesterase (PDE) inhibitor whose potency is in the micromolar level for all isoforms of PDEs; however, some of the potency is in nanomolar concentrations against PDE5 [28–30]. We have modified this molecule to generate mammalian PDE5 isoform-specific activity [22,31,32]. One modification involved the 8-position of IBMX to shift the non-specific inhibitor into a more specific non-mammalian cAMP-binding PDE to avoid unnecessary interference with human PDE function (unpublished data). As expected, the newly generated analogs were very potent on PDE1 and, more specifically, PDE5. Though it has been reported that *T. cruzi* expresses PDEs that bear homology to the mammalian PDE family [22], one variant of *T. cruzi* PDE, TcrPDEC, has an affinity to both cAMP and cGMP and has been proposed as a potential drug development target at the micromolar range [23,33].

Based on this knowledge, we screened the xanthine analogs that were originally developed as mammalian PDE5 inhibitors. Our screening study identified several molecules that inhibited *T. cruzi* infection in nanomolar concentrations. Because of the high genetic and phenotypic intraspecific diversity in *T cruzi*, it has been classified into about seven discrete typing units (DTUs), named TcI to TcVI and Tcbat [34–36]. Anti-trypanosomal drugs act by damaging DNA, and the reactive metabolites are generated via the reductive metabolism regulated by *T. cruzi* flavin-dependent mitochondrial type 1 nitroreductase (TcNTR-1) [37]. One of the active molecules was tested on various drug-resistant strains and shown to be highly potent in all strains. This study demonstrates that novel selective inhibitors of *T. cruzi* PDEs could be further developed for Chagas disease.

2. Materials and Methods

2.1. Synthesis of Xanthine Analogs

Xanthine analogs with phenylthio substitution were synthesized with a slight modification of the methods described in the literature [28]. 8-bromo-IBMX was stirred with substituted thiophenols in methanol in the presence of sodium acetate and trace amounts of water. The 8-substituted benzyl-IBMX, 8-substituted cycloalkylmethyl-IBMX, and 8-substituted styryl-IBMX analogs were synthesized by reacting 1-isobutyl-3-methyl-5,6-diaminouracil with substituted phenylacetic acids, alicyclic carboxylic acids, and substituted cinnamic acids, respectively. The two reagents were stirred overnight with condensing agent 1-(3-

dimethylaminopropyl)-3-ethylcarbodiimide hydrochloride. Sodium hydroxide (2M) was heated at 90 °C for 2 h to obtain the products [23]. A similar approach was used to prepare theophylline analogs. All compounds were purified either by recrystallization or by column chromatography using silica gel. The pure trans isomer of 8-(4-chlorostyryl)-IBMX was synthesized by reacting commercial trans 4-chlorocinnamic acid with 1-isobutyl-3-methyl-5,6-diaminouracil in the dark. Cis isomer was obtained by exposing a methanolic solution of trans isomer to light for 1 week. Cis isomer was separated from the trans isomer by HPLC (Whatman Partisil M20 10/25 ODS-3, mobile phase CH_3CN:water (7:3)). Based on previous work examining the structures of selective inhibitors of PDE-5, confirmed by NMR, mass spectroscopy, and elemental analysis, the xanthine analogs that were synthesized included functional groups and residues that inhibited PDE-5 via molecular interactions [38,39].

2.2. Rat Heart Myoblast Culture

Rat heart myoblasts (RHMs) were obtained from ATCC Inc. and maintained by incubating at 37 °C with 5% CO_2 in DMEM containing glutamax (Life Technologies, Carlsbad, CA, USA) by supplementing with 10% heat-inactivated fetal bovine serum (Life Technologies), 1% penicillin/streptomycin (Life Technologies, Carlsbad, CA, USA) and 1% non-essential amino acid and MEM-vitamin (Life Technologies, Carlsbad, CA, USA).

2.3. Parasites

Based on genetic variability, *T. cruzi* is classified into about 7 DTUs; high genetic diversity, along with the multi-clonality of the natural population, has led to various levels of drug resistance against the clinically approved drugs [40–42]. Three strains Tulahuen, Y, and CA-1 CL72, were used in this study based on their drug resistance to benznidazole and nifurtimox. The Tulahuen strain (20A clone) is a highly invasive tryomastigote clone derived from a heterogeneous population of the Tulahuen strain of blood trypomastigotes, with different degrees of infectivity, originally isolated in Tulahuen, Chile [43]. The Y strain, isolated from a Chagas disease patient in Belo Hrizonte, Brazil, was obtained from ATCC (ATCC 50832) [44]. The CA-CL72 strain is a Nifurtimox-resistant strain obtained from ATCC (ATCC 50791) [45], originally isolated from a human male with chronic myocarditis in San Luis, Argentina, and cloned by J. Dvora from NIH in 1980. These strains have different drug susceptibility and geographic distribution as drug resistance have been observed in natural populations of *T. cruzi* strains without prior exposure to drugs [46]. Both Y and CA-1 CL72 were received as epimastigotes and grown in liver transfusion media (LIT) with 10% fetal calf serum (FBS) and hemin [47]. Further, infective trypomastigotes forms were obtained by infecting the cells in vitro. Trypomastigotes expressing green fluorescent protein (GFP) were generated as described previously [48].

2.4. Trypanosomes Expressing Green Fluorescent Protein (GFP)

Pure cultures of *T. cruzi* trypomastigotes expressing GFP were obtained from the supernatant of heart myoblast monolayers, as described previously [48–51]. Amastigotes expressing GFP were obtained by originally infecting Vero cells with trypomastigotes expressing GFP, and growing amastigotes-GFP in cell-free medium, as described [52].

2.5. GFP-Expressing Amastigote Forms in a Cell-Free Medium

Amastigotes were obtained from the GFP-expressing trypomastigotes released from myoblasts, as described earlier by Villalta et al. [52,53]. Amastigotes were axenically grown in DMEM media with 10% FBS for 3–5 days and seeded at 1×10^6 parasites per well in a 24/48 well plate.

2.6. T. cruzi Trypomastigote Culture and Infection Assays

RHMs were used to generate trypomastigotes and amastigotes from the 3 strains. To generate the trypomastigotes, cells were grown to 80% confluence, followed by incubation with infective *T. cruzi* trypomastigotes expressing GFP [46,52,53]. Highly infective

(infect >95% of cells) *T. cruzi* trypomastigotes were harvested from tissue culture supernatants and washed with Hanks Balanced Salt Solution (HBSS) and further used for the drug infection studies. After 20–24 h of infection, uninfected parasites in the media were washed off to prevent prolonged infection with $1\times$ DPBS (without calcium/magnesium), and various concentrations of PDE inhibitors (1 nM to 100 nM) were added. DMSO (10 µL) was used as solvent control, with a similar volume of the dissolved compounds, and benznidazole (2.5 u) was used as a positive control under similar conditions [42,54]. Monolayer cells were further incubated with the inhibitors for 36 h, just before the first batch of release of the trypomastigotes from the host cells, and washed twice with 1XPBS to remove the unbound trypomastigotes. To measure the PDE inhibitory action using relative florescent units (RFUs), cells were incubated in Phenol-Red-free DMEM media for 24 h and GFP intensity was measured using a spectrophotometer (BioRad Inc., Hercules, CA, USA)with a single excitation peak centered at about 488 nm, with an emission peak wavelength of 509 nm.

2.7. Florescent Microscopic Assays

After treating the cells with respective concentrations of PDE inhibitors, cells were fixed with 2.5% paraformaldehyde (*w/v*) for 5 min at room temperature, followed by washing with $1\times$ DPBS, and perforated with 0.1% Triton-X100 in PBS for 5 min. Cells were blocked with 3% BSA-PBS for 30 min at room temperature. Alexa fluor 546 phalloidin (Invitrogen) was used at a ratio of 1:2000 to visualize cardiomyocyte actin myofibrils, as described previously [52,53], and the nucleus was stained with 4′,6-diamidino-2-phenylindole (DAPI, Thermofisher Inc., Waltham, MA, USA). Stained cells were analyzed for compound inhibition using a Nikon A1R confocal microscope, and images were captured by imaging software NIS Elements AR Analysis version 5.20.02 64-bit.

2.8. Treatment of Amastigotes with PDE Inhibitors

Amastigotes were treated with 50 nM of PDE inhibitors or DMSO as control for 4 days. RFU was determined every 24 h for 4 days of treatment by fixing the amastigotes with 2.5% formaldehyde. Amastigotes were observed under confocal microscopy (Nikon A1R model). The software used for the analysis was NIS Elements AR 5.30.05, using the channels FITC (488; 500–550).

2.9. Annexin V Assay

The annexin V assay was used to detect the apoptosis induced by the xanthine analogs via the detection of translocated phosphatidylserine from the inner to the outer leaflets of the plasma membrane. Further treatment with propodeum iodide (PI) detected dead cells with permeabilized plasma membranes. The experiment was performed according to the manufacturer's instructions using the Alexa Fluor488 Annexin V/Dead Cell Apoptosis Kit (Thermo Fisher Scientific Inc., Waltham, MA, USA). RHM cells were treated with 100nM of xanthine analogs for 48 h. After treatment, detached as well as adherent cells were washed twice with cold 1XPBS. The cell pellet was resuspended in 100 µL of annexin-binding buffer at a density of 1×10^4 cells per ml and incubated with 5 µL of Alexa-488-conjugated annexin V and 5 µL of PI for 15 min at room temperature in the dark. About 400 µL of binding buffer was added to each sample tube, and the samples were immediately analyzed by flow cytometry. Histograms and statistics were analyzed using the software FlowJo Version 7.6.5.

2.10. Cell Cytotoxicity Assay Using CCK-8

RHM cells were counted and seeded into a 96-well culture plate at a concentration of about 5000 cells per well (TPP Inc., Pierceton, IN, USA). Cells were further incubated at 37 °C in a humidified incubator under 5% CO_2 for 24 h; the medium was replaced and washed 2 times with $1\times$ PBS and replaced with media contacting 100 nM of IBMX analogs along with a corresponding volume of DMSO (10 µL) as control. The plates were further

incubated for 48 h in the CO_2 incubator at 37 °C. A replicate of three measurements was made for each group. Finally, 10 µL of CCK-8 reagent (MedChemExpress Ltd., Monmouth Junction, NJ, USA) was added to each well, and OD at 450 nm was measured using a BD Biosciences Multiplate Reader (BD Biosciences, Inc., Haryana, India) after incubation for 2 h at 37 °C. Values were calculated and normalized in Microsoft Excel, and graphs were plotted in Graphpad Prism.

2.11. Selectivity Index

RHM cells, about 10,000 cells per well, were seeded into 48-well plates (TPP Inc., Pierceton, IN, USA), and further incubated at 37 °C in a humidified incubator under 5% CO_2 for 24 h. The medium was replaced and washed 2 times with $1\times$ PBS and replaced with media contacting various concentrations of IBMX analogs, ranging from 1 to 100 uM; similar treatments were also performed on RHM cells infected with *T cruzi*, as mentioned above. The selectivity index was determined by calculating the IC50 value ratio between the uninfected vs. infected RHM cells.

2.12. cAMP ELISA

Trypomastigotes expressing GFP were treated with PDE inhibitors for 48 h, followed by centrifugation at 3000 RPM for 15 min. The supernatants were obtained for the analysis of secreted cAMP levels. *T. cruzi* trypomastigotes were suspended at a concentration of 1×10^8 cells per ml and incubated with or without PDE inhibitor for 10 min in PBS supplemented with 5 mM glucose. Aliquots of 0.5 mL were taken at 1 and 5 min post-incubation, centrifuged, and resuspended in 100 µL of PBS and 400 µL of 50 mM sodium acetate, pH 5.5, preheated to 95 °C. The samples were then heated at 95 °C for 5 min, after which the samples were centrifuged and the supernatants were collected and stored at -20 °C. The cAMP levels were measured at the 420 nm wavelength using a spectrophotometer (BioRad Inc., Hercules, CA, USA) and analyzed per the protocol of the cAMP ELISA kit (Cayman Chemicals, Ann Arbor, MI, USA).

2.13. Chemical Absorption, Distribution, Metabolism, Excretion, and Toxicity (ADMET) Levels and Scoring

ADMET properties are one of the essential criteria for the assessment of a drug-like nature. We evaluated the chemical drug-likeness of the xanthine analogs using admetSAR online software [55]. Individual chemical compounds were drawn to obtain the SMILES, which were then used to predict the chemical absorption, distribution, metabolism, excretion, and toxicity levels of the xanthine analogs. admetSAR allows for the calculation of pertinent ADMET properties using binary and non-binary classification models. Binary-classified properties such as Ames mutagenicity (Ames), acute oral toxicity (AO), Caco-2 permeability (Caco-2), P-glycoprotein substrate (P-gps), P-glycoprotein inhibitor (P-gpi), CYP substrates and inhibitors (CYP1A2, CYP2C9, CYP2D6, CYP2C19, and CYP3A4), human intestinal absorption (HIA), CYP inhibitory promiscuity (CYPPRO), carcinogenicity (CARC), human ether-a-go-go-related gene inhibition (hERG), and the organic cation transporter protein 2 inhibitor (OCT2i) were calculated. Ternary- or quaternary-classified properties such as chemical carcinogenicity and acute oral toxicity were transferred into binary prediction models.

2.14. Chemical Diversity Measurement

We evaluated the chemical diversity of the xanthine analogs using ChemMime online software [56]. Using the canonical SMILES of individual chemical compounds generated with admetSAR, we utilized a hierarchical clustering method that uses the hclust function implemented in R to calculate the chemical similarity across all xanthine analogs. We employed the single linkage rule in our hierarchical clustering scheme using the distance matrix of all-against-all compound distances that is generated by subtracting the Tanimoto coefficient Tc (which is defined by the proportion of features shared among two compounds

divided by their union) from 1 (1–Tc) to determine structural diversity among our xanthine compounds.

3. Results

Xanthine Structural Modifications and Activity against T. cruzi

The xanthine base structure was modified at various positions to understand the structural requirements needed for the effective inhibition of *T. cruzi* (Figure 1). Xanthine base structure substitution occurred with thiophenols, phenylacetic acids, salicylic carboxylic acids, or substituted cinnamic acids (Figure 1). The compounds were confirmed by NMR, mass spectroscopy, and elemental analysis. The IC50 values of the analogs were determined against the mammalian PDEs. Phosphodiesterases were purified, and assays were performed as described earlier. These PDEs include both cGMP- and cAMP-specific PDEs [57,58].
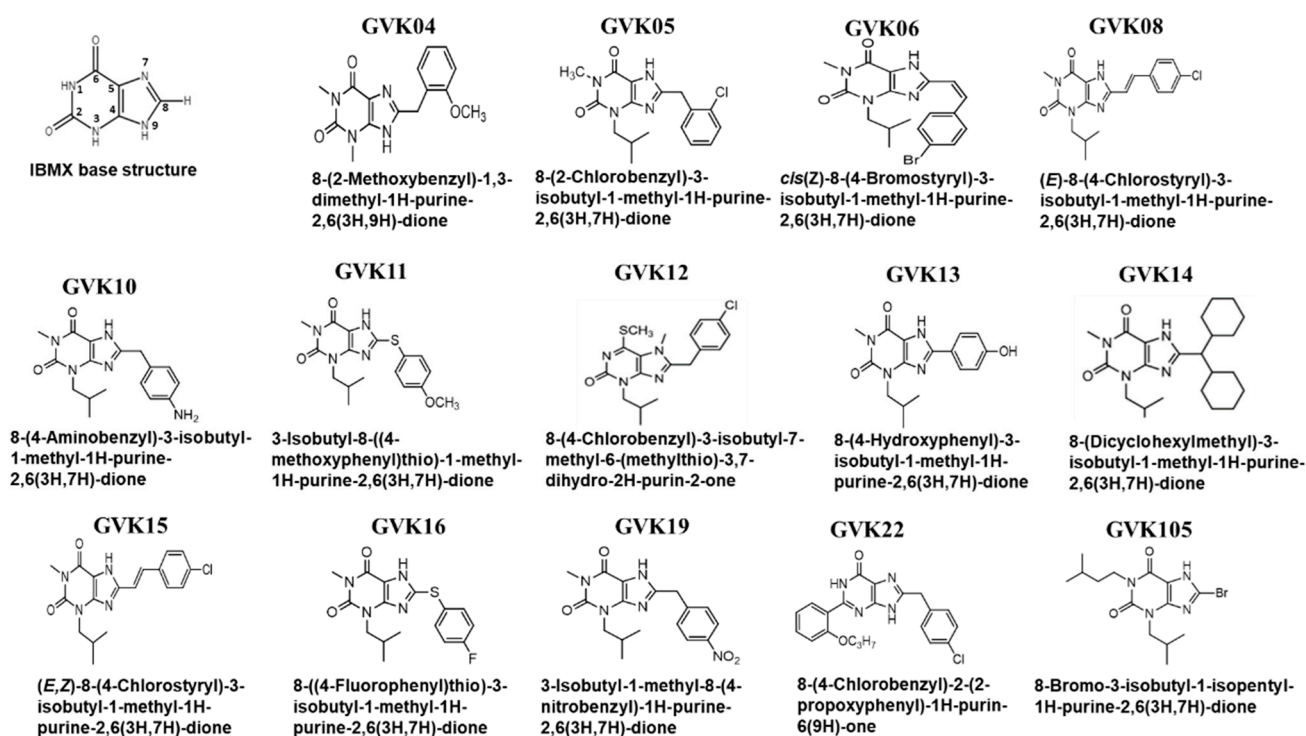

Figure 1. Synthesis of xanthine compounds and modifications: The figure represents the schematic illustrating the xanthine base structure of IBMX, where the numbers 1 to 9 represent the possible modification locations. Several analogs were synthesized based on the xanthine structure of IBMX.

Stable GFP-expressing trypomastigotes (Tulahuen strain) were generated using the myoblasts. Trypomastigotes were collected after the second release, in which higher numbers of the single form of parasites could be found. The inhibitor evaluation experiments were performed in 24-well plates in triplicate at an infection ratio of 10 parasites per cell after 24 h of infection; cells were washed to remove the unbound trypomastigotes, and RHMs were treated with several modified compounds to evaluate the efficacy of the inhibitors. Several molecules, GVK 14, 16, 19, and 22, decreased the growth of amastigotes inside the infected cells compared to solvent control, DMSO (Figure 2A). The green fluorescence intensity was measured and is represented as RFUs in the graph (Figure 2B), where the RFUs are compared to the DMSO control. To further rule out the toxicity of the drugs to the host cells, we performed FACS analysis of the cells that were treated with annexin V staining, along with PI staining, to determine quantitatively the cells undergoing apoptosis. To determine the viability of cells during the inhibitor treatment, PI staining was used. The cells positive for FITC annexin V, negative for PI, or positive for FITC annexin V/positive

for PI were undergoing apoptosis or at the end stage of apoptosis, respectively. It was found that the inhibitor-treated cells presented negative staining for both FITC annexin V and PI and were not undergoing apoptosis, indicating that the inhibitors are not toxic to the cells. The xanthine analogs showed no toxicity in the host cells (Figure 2C). The cells were also checked for the cytotoxicity effect of the Xanthine analogs using the CCK-8 assay, where the RHM cells were treated with the highest concentration of the analogs, 100 nM, for 48 h and cell viability remained over 80% after treatment with various xanthine analogs (Figure 2D).
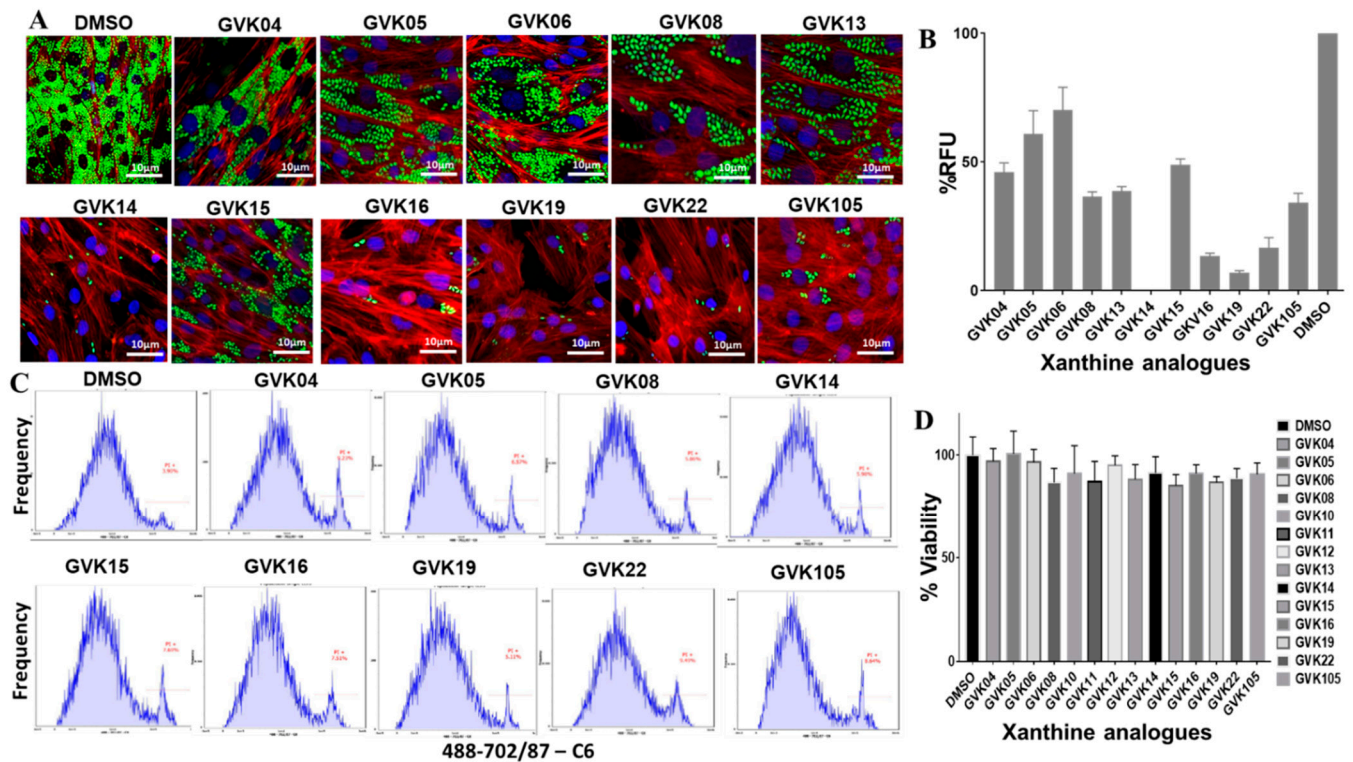

Figure 2. IBMX analogs inhibit *T. cruzi* infection in vitro. (**A**) Fluorescent microscopic images of RHM infected with *T. cruzi* (Tulahuen strain) expressing GFP. RHMs were treated with 50 nM of IBMX analogs, and parasite infection was evaluated after 24 h. Green fluorescence represents actively growing *T. cruzi* amastigotes inside the cells. (**B**) Graphs were created based on green fluorescence intensity, which is measured as % RFU intensity, and DMSO control is shown as 100%. (**C**) FACS analysis of the infected cells with the respective inhibitors represents cellular toxicity using annexin V-PI staining. (**D**) CCK-8 assay for cell viability or cytotoxicity after treatment with 100 nM of xanthine compounds on RHM cells. Data are analyzed as mean $\pm$ standard deviation (SD) (n = 3) for CCK-8 assays.

Cellular cytotoxicity selectivity was also determined by measuring the selectivity index values of the analogs. The ratio values ranged from 1 to 1.33 (Table 1 and Table S1), which represent less toxicity to the RHM cells when infected.

Table 1. EC$_{50}$ and selectivity index of GVK14 in infected myoblasts by strains of *T. cruzi*.

Strain	GVK14 (nM)	SI
Tulahuen	2.4 ± 0.2	$15,833.3 \pm 620$
Y	3.6 ± 0.5	$10,555.55556 \pm 800$
CA-1 CL72	2.8 ± 0.8	$13,571.42857 \pm 1000$

The ADMET analysis was performed based on the definition of the ADMET score presented above in the Methods section (Tables 2 and S2). The canonical SMILES of analogs, molecular weight, and A log P (Ghose–Crippen Log K_{ow}), as well as the logS prediction values of ADMET properties, are listed in Table S2. ADMET scores of each compound were predicted using the software admetSAR 2.0. The chemical space distribution of the compounds is shown graphically in Figure 3, along with the water solubility (Figure 3A,B). The A log *P* ranged from −1 to 4.4. This data demonstrates that most of the xanthine analogs are highly hydrophobic in nature. We further measured the chemical diversity of the compounds using the ChemMime software. Figure 3C,D show the distribution of molecular weight (MW) and Tanimoto similarity. As shown in Figure 3C, the MW of the xanthine analogs ranges from 152 to 400. The heat maps of the Tanimoto similarity matrix show the shared structural identity in these molecules (Figure 3D), which is expected as they are derived from the parent xanthine structure. GVK14 showed high absorption, distribution, metabolic activity, and excretion and lower toxicity in various organs (Tables 2 and S2).

For the consideration of drug-likeness, we assessed only the appropriate criteria, excluding endpoints that were related to environmental risk. However, we kept those in the data presented in Table S2 because of the significance of eco-toxicity models, along with other pertinent endpoints. We evaluated the bioavailability of the xanthine analogs using predictive models within admetSAR2.0 that estimated the movement of the molecules across the intestinal epithelial barrier. For GVK14 and the majority of the other xanthine analogs, the rate and extent of human absorption predicted in the human intestinal absorption (HIA), human oral bioavailability (HOB), and Caco-2 permeability values were positive, showing the likelihood of drug absorption. We also determined the estimated distribution of xanthine analogs by P-glycoprotein (P-gp), a key transporter protein involved in drug distribution and many essential processes related to drug pharmokinetics [59]. GVK14, along with the majority of the other xanthine analogs, show minimal cytochrome P450 (CYP) promiscuity; that is, they do not inhibit P-gp or serve as a substrate for P-gp. This signifies that the distribution of the xanthine analogs will not be hampered. *T. cruzi* presence has been reported in glial cells, and the acute phase of infection can cause severe nervous system complications, including meningoencephalitis, which frequently occurs in children before 2 years of age [60]. Hence, we predict the blood–brain penetration capabilities of the xanthine analogs. All the xanthine analogs studied are predicted to have the ability to cross the blood–brain barrier. We further investigated the possibility of clinical drug–drug interactions with other drugs using the predictive model by assessing the inhibition of CYP enzymes, particularly isoforms 1A2, 2C9, 2C19, 2D6, and 3A4, which are responsible for about 90% of oxidative metabolic reactions [61]. GVK14, along with the majority of the other xanthine analogs, show minimal CYP promiscuity; that is, they do not inhibit multiple CYP isoforms and, thus, will not likely be involved in drug–drug interactions with various other drugs but will be metabolized in the body. In addition, using admetSAR2.0, we measured the likelihood of GVK14 and all other xanthine analogs accumulating in the kidney or being excreted by predicting whether they serve as organic cation transporter 2 (OCT2) inhibitors. OCT2 is the initial step in the renal secretion of many cationic drugs [58]. Finally, we predict the overall toxicity of the xanthine analogs using the various toxicity endpoints within admetSAR2.0 prediction models. GVK14 and other xanthine molecules have shown some level of predicted toxicity. We evaluated the Ames mutagenicity, which looks at the potential for teratogenicity and genotoxicity in the early stages of drug discovery. GVK14 and the majority of the other xanthine molecules were negative for Ames mutagenicity. Another major area for predicting toxicity is the inhibition of the human ether-a-go-go-related gene (hERG) potassium channel. Inhibiting hERG can cause severe cardiac side effects due to prolonged QT intervals [62]. GVK14 and many of the other xanthine analogs show this possibility. Very importantly, acute oral toxicity and carcinogenicity are very crucial toxicological endpoints. The majority of the xanthine analogs are in category III, which represents slightly toxic and slightly irritating molecules.

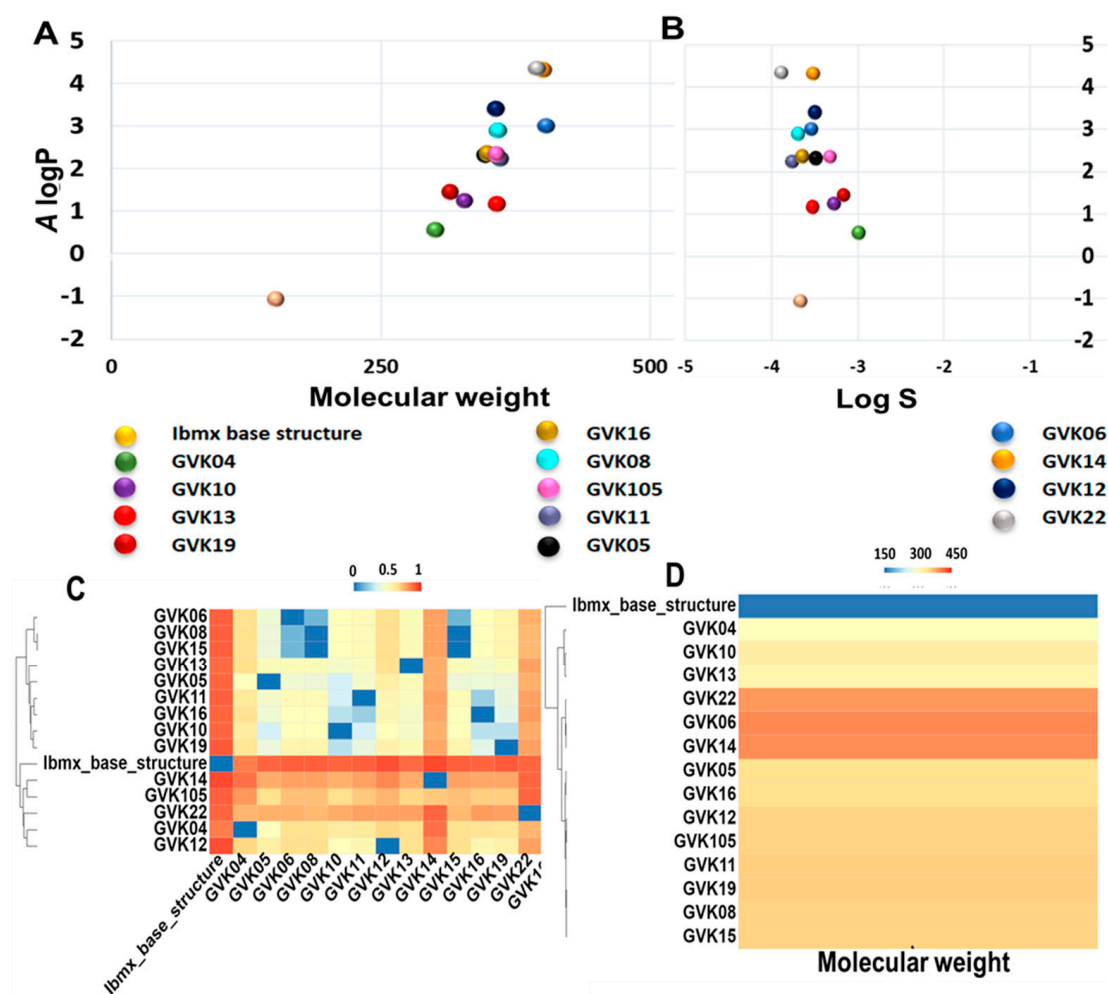GVK14 shows moderate toxicity in category II. All these compounds are predicted to be non-carcinogenic.

Figure 3. Distribution of chemical properties on xanthine analogs. Panel (**A**): Chemical space distribution of xanthine analogs. Chemical space is defined by molecular weight (MW) as the *X*-axis and Ghose–Crippen Log K_{ow} (*A* log *P*) as the *Y*-axis. Panel (**B**): Ghose–Crippen Log K_{ow} (*A* log *P*) (lipophilicity) versus aqueous solubility (log S). Panel (**C**): The molecular weight distribution of the xanthine analogs used in this study. Compounds with similar molecular weight are closer in color. Panel (**D**): Tanimoto similarity index for all xanthine analogs used in this study; colors closer to red in the heat map mean that the compounds are more similar, and colors closer to dark blue mean that the compounds have higher diversity.

For the purpose of therapeutic convenience, it is of utmost importance to validate whether these molecules inhibit other strains of *T. cruzi*. Hence, we tested the most potent molecule identified in our screening, GVK14, on three strains of *T. cruzi* (Tulahen, Y, and CL72). The antiparasitic activity of GVK14 against the three strains of *T. cruzi* was analyzed in amastigotes, the most clinically relevant, intracellular form of the parasite, by quantifying the rate of multiplication within the infected cardiomyocytes (Figure 4).

Table 2. ADMET properties prediction of xanthine analogs.

		IBMX Base	GVK 04	GVK 05	GVK 06	GVK 08	GVK 10	GVK 11	GVK 12	GVK 13	GVK 14	GVK 15	GVK 16	GVK 19	GVK 22	GVK 105
A (Absorption)	Human intestinal absorption (HIA)	+	+	+	+	+	+	+	+	+	+	+	+	+	+	+
	Human oral bioavailability (HOB)	+	+	-	+	+	+	-	-	-	+	+	+	-	+	+
	Caco-2 permeability	-	+	+	+	+	+	+	+	+	-	*	+	+	-	+
D (Distribution)	Blood–brain barrier penetration (BBB)	+	+	+	+	+	+	+	+	+	+	+	+	+	+	+
	P-glycoprotein inhibitor (P-gp)	-	-	-	-	-	-	-	+	-	-	-	-	-	+	-
	P-glycoprotein substrate	-	-	-	-	-	-	-	-	-	-	-	-	-	-	-
M(Metabolism)	CYP inhibitory promiscuity	-	-	-	+	+	-	+	-	-	-	+	-	-	+	-
E (Excretion)	OCT2 inhibitor	-	-	-	-	-	-	-	-	-	-	-	-	-	-	-
	Acute oral toxicity (log(1/(mol/kg)))	III: 2.611	III: 2	III: 2.632	III: 2.919	III: 2.777	III: 3.275	III: 2.607	III: 3.19	III: 2.55	II: 2.934	III: 2.777	III: 2.998	III: 2.902	III: 2.045	I: 3.174
T (Toxicity)	Human either-a-go-go-ralted gene (hERG) inhibition	-	+	+	+	+	+	+	+	-	-	+	+	-	+	-
	Ames mutagenesis	-	-	-	-	-	+	-	-	-	-	-	-	+	-	-
	Carcinogenicity (binary)	-	-	-	-	-	-	-	-	-	-	-	-	-	-	-

The dose–response curves indicated that the compound had remarkable antiparasitic activity, clearing Tulahuen, Y, and CA-1 CL72 *T. cruzi* infections at low nanomolar concentrations. After 72 h of infection, the cardiomyocyte monolayers were washed with PBS, and the infection was fluorometrically quantified as relative fluorescence units (RFUs). The EC50 values were 2.4, 3.6, and 2.8 nM for *T. cruzi* strains Tulahuen, Y, and CA-1 CL 72, respectively (Figure 4B, Table 1). As the positive control, benznidazole (50 nM) was used (Figure 4B). Compared to the control drugs, GVK14 showed effective inhibition of the amastigotes' growth in all three strains of *T. cruzi* (Figure 4A).

Effect of PDEs on the growth of amastigotes:

The xanthine analogs efficiently inhibited the extracellular amastigotes and also inhibited intracellular amastigote proliferation. To further characterize and differentiate between intracellular and extracellular amastigote proliferation in the drug screening assay, we further determined the cytotoxicity effect of the inhibitors by targeting the axenically growing amastigotes. We treated the axenically growing amastigotes with the inhibitors for 24 to 72 h. As expected, the inhibitor GVK14 successfully inhibited the growth of amastigotes within 24 h, while the control amastigotes continued to grow exponentially for 4 days (Figure 5A). Confocal microscopic images showed that the axenic culture of stable GFP-expressing Tulahuen-strain amastigote proliferation was inhibited by the treatment with GVK14 (Figure 5C) compared to that of the DMSO control (Figure 5B).

Cyclic AMP determinations: To validate that these xanthine analogs inhibit the *T. cruzi* PDEs and inhibit the growth of the log-phase, we determined the cAMP levels in *T. cruzi* at a single dose of 50 nM. Most of the active molecules increased cAMP levels significantly, suggesting that these IBMX analogs inhibit PDEs of *T. cruzi*. GVK14 induced highly significant levels of cAMP, followed by GVK19 and -22 (Figure 6A; Table 3) compared to DMSO-treated myoblasts. To evaluate the selectivity of action or to determine xanthine analog activity against mammalian PDEs, we treated the RHM cells with the compounds at 50 nM concentrations for a period of 48 h, and cAMP levels were measured. The cAMP levels were not changed compared to control untreated cells. The correlation coefficient was calculated to determine the relationship between two dependent variables, and the

potency of drugs and secreted cAMP levels were investigated; none of these levels were chosen a priori. Upon the Pearson correlation coefficient calculations, the r-value of the xanthine analogs was −0.67, which shows a negative correlation, which explains our results as these analogs are in a negative relationship.
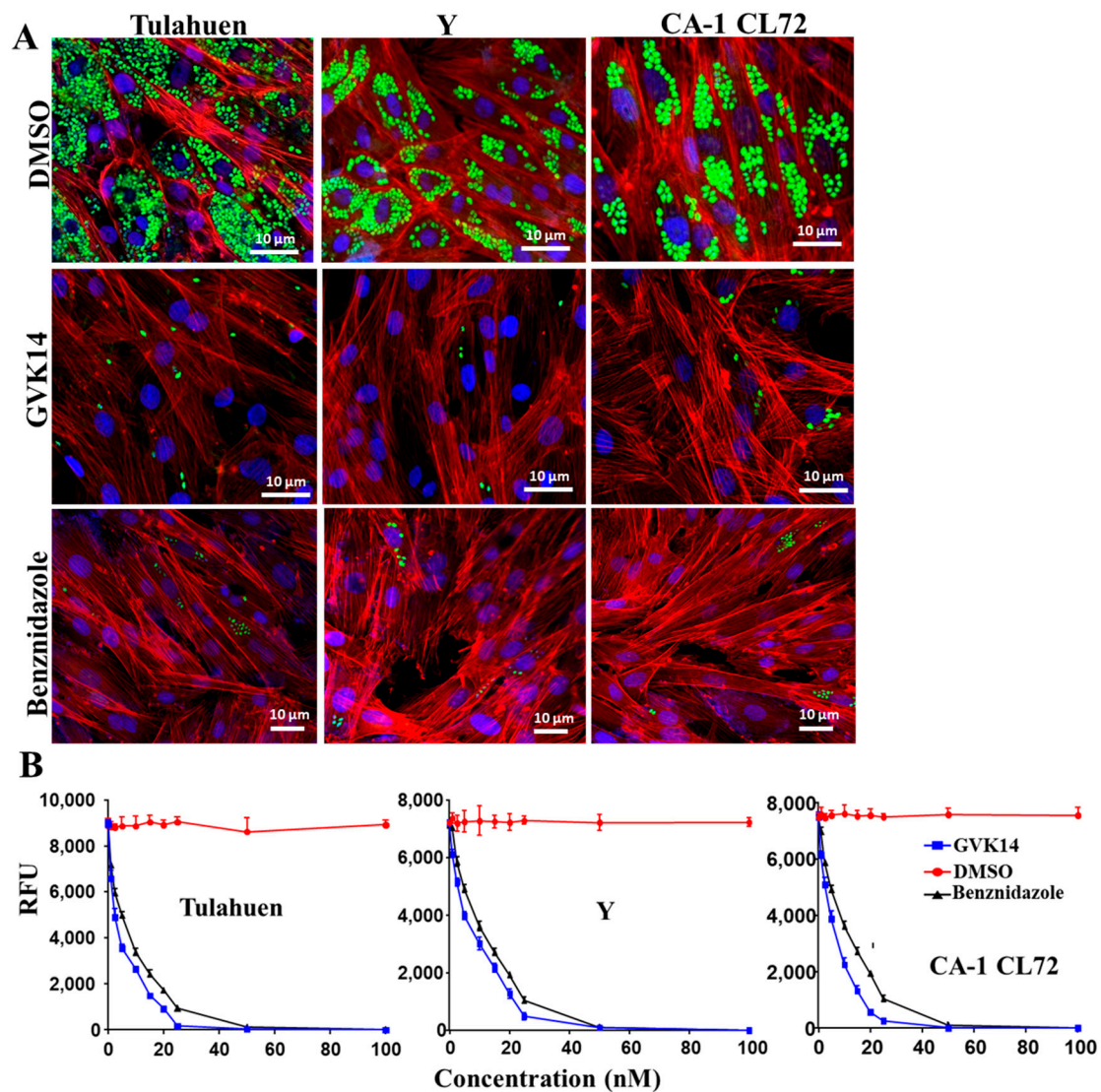

Figure 4. Effect of compounds on actively growing amastigotes in heart myoblasts infected with three *T. cruzi* strains. (**A**) RHM infected with GFP-expressing trypomastigote clones of Tulahuen, Y, and CA-1CL72 strains (infection of 10 parasites per cell) after 24 h of infection and then treated with GVK14 (50 nM) or, as positive control, benznidazole (50 nM) or DMSO. Green color represents *T. cruzi* amastigotes; blue represents cardiomyocyte nuclei; red is myoblast actin myofibrils. (**B**) Line graph depicting dose-dependent suppression of the Tulahuen, Y, and CA-1 CL72 strains expressed as relative fluorescence units (RFUs) at 72 h are shown. All experiments were performed in triplicate, and the results are presented as means ± SEs. Statistical analysis was performed by two-way ANOVA, $p < 0.05$.
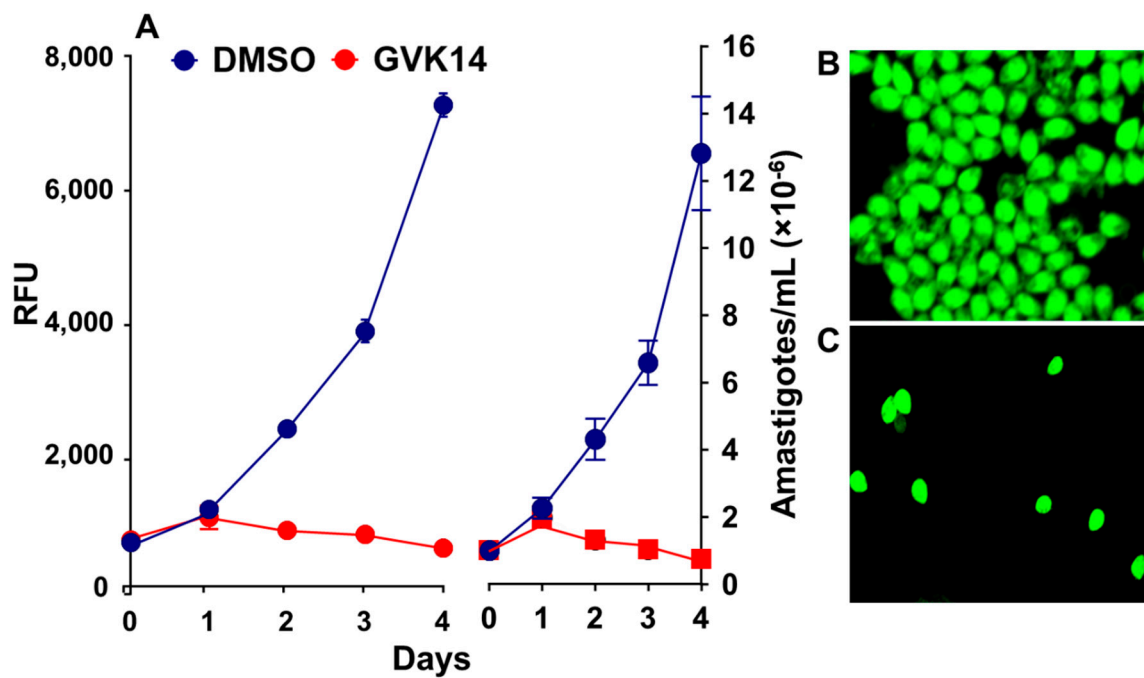
Figure 5. Inhibitor effects on the axenic growth of cloned amastigotes-GFP in cell-free medium. (**A**) Effects of GVK14 on the growth of cloned amastigotes-GFP evaluated by RFUs. (**B,C**) Growth of amastigotes-GFP treated with DMSO and GVK14 was evaluated microscopically.
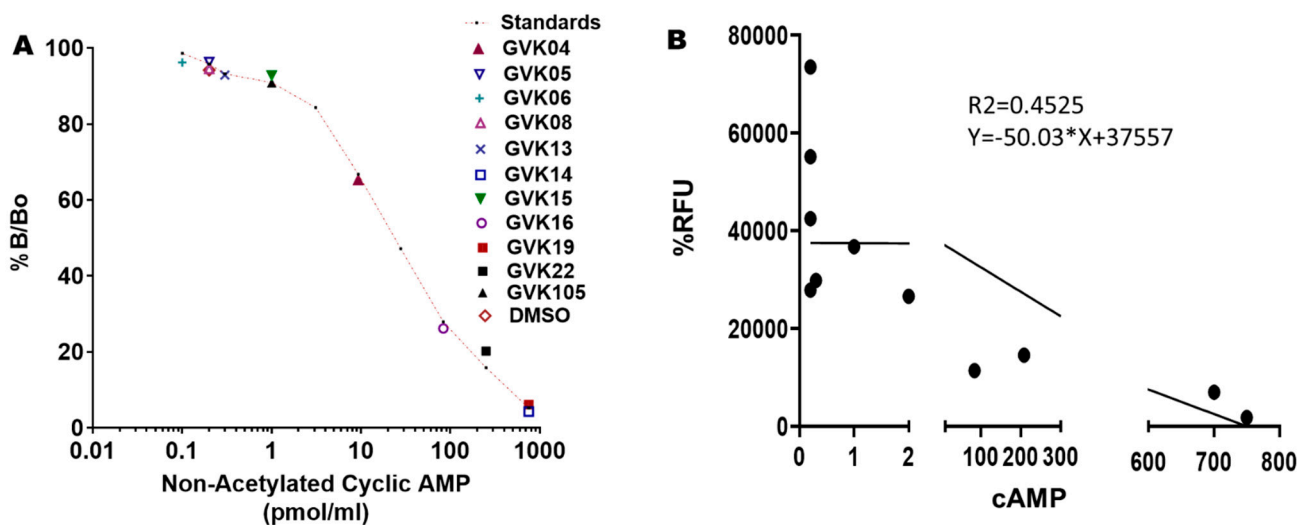

Figure 6. Changes in secreted cyclic AMP (cAMP) levels with the treatment of PDE inhibitors. **Panel** (**A**): cAMP levels were measured using the Cayman ELISA kit after treating the Tulahuen strain of *T. cruzi*. The red-lined graph represents the standards of the cAMP provided by the manufacturer. All experiments were performed in triplicate, and the results are presented as means ± SEs. This is a competition assay, and the levels of secreted cAMP are shown on the X-axis. Statistical analysis was performed by two-way ANOVA, $p < 0.05$. **Panel** (**B**): Represents the correlation graph that shows the treatment of analogs on RHM cells compared with the secreted cAMP levels. Graphs were created based on green fluorescence intensity, which is measured as % RFU intensity; DMSO control is shown as 100%. The 95% CI is −0.8994 to −0.1609, with a Pearson's r-value of −0.67.

Table 3. Values of cAMP levels (pmol/mL) secreted in *T. cruzi* with respective xanthine analogs.

IBMX	cAMP pmol/mL
GVK04	9.3
GVK05	0.2
GVK06	0.2
GVK08	0.2
GVK10	3.1
GVK11	3.1
GVK12	9.3
GVK13	0.3
GVK14	750
GVK15	1
GVK16	84
GVK19	700
GVK22	208
GVK105	2

4. Discussion

T. cruzi, the etiological agent of Chagas disease, expresses several phosphodiesterases (PDEs) that have shown homology to many human PDEs [24]. TcPDE1, a novel membrane-bound PDE that is associated with flagellum, has significant homology with the *T. brucei* TbPDE2 family [17]. TcPDE4 also shows significant homology to the PDE4 family of enzymes, which possess a high affinity for cAMP [18]. These findings prompted us to screen inhibitors of PDEs, specifically IBMX analogs, as possible drugs for the treatment of Chagas disease. Xanthine analogs and xanthine-containing molecules have been previously identified as possible drugs for Chagas disease [63]. However, due to the unknown mechanism of action of these complex xanthine analogs and the high cost of synthesis, further development of these molecules was abandoned. In the current study, we have designed simple xanthine analogs with known mechanisms of action that could reduce the cost of synthesis.

IBMX analogs possess anti-inflammatory, anti-aggregating, and anti-hypertensive properties [64]. These IBMX analogs are known to inhibit various forms of PDEs by interfering with the different signaling pathways that enhance the cAMP levels, which increase cellular nucleotide levels, osmoregulation, and cytokinesis levels [16]. These compounds may also act on cAMP-dependent immune suppressive mechanisms.

IBMX, a non-specific PDE inhibitor with micromolar potency [28], has been modified to mimic cAMP/cGMP by adding a substitution at the 8-position of the molecule. This substitution is believed to mimic ribose cyclic phosphate groups present on cAMP/cGMP molecules [64]. Although these molecules were designed to target mammalian PDE5, the IBMX moiety could be accommodated in the cyclic nucleotide-binding site of the parasite's PDEs [28,64].

We introduced several substitutions at the 8-position that could provide substitution preference by the cyclic nucleotide-binding site of the PDEs. These include substituted benzyl, substituted phenylthiol, and substituted phenyl groups. We have also modified substitutions at the 1-, 2-, 3-, and 6-positions of the molecule to understand the structural requirements, and we introduced a substitution found in one of the earlier cGMP-PDE inhibitors, zaprinast [65]. Interestingly, many molecules have shown significant activity in reducing the infection of *T. cruzi*. Substitutions with both electron-withdrawing and electron-donating groups showed activity, suggesting that the catalytic cyclic nucleotide-binding site in the TcPDE has ample space to orient the molecule and interact with various parts of the molecule.

The most potent among these molecules was GVK14, with 97% inhibition of infection by parasites. A dicyclohexylmethyl substitution at the 8-position of IBMX was induced in GVK14. This substitution is highly hydrophobic in nature. Interestingly, mammalian PDE5 has a preference for hydrophobic substitutions at the 8-position of IBMX [28]. This

observation might suggest that the cyclic nucleotide-binding pocket of *T. cruzi* PDE has a hydrophobic interaction site. Similarly, GVK19, which has a nitro group at the 4-position of benzyl substitution, showed potent inhibition of *T. cruzi* infection. Electron-withdrawing groups on benzene substitution were not tolerated by mammalian PDE5. Electron-donating groups, such as hydroxy and amino groups, as well as halogen substitution on benzene substitution, were well tolerated by mammalian PDE5 and *T. cruzi* PDEs. It is noteworthy that both electron-withdrawing and electron-donating groups on IBMX analogs were equally favored by *T. cruzi* PDEs. One of the molecules introduced was a propoxyphenyl group (GVK22) that was found in the cGMP-specific PDE inhibitor zaprinast. GVK22 was also found to be a potent inhibitor of *T. cruzi* PDEs, suggesting that possible modifications could be made at the location of the isobutyl group (3-position of IBMX) in IBMX. A modification with a trans-styryl group at the 8-position of IBMX reduced the potency of the molecule, which is similar to mammalian PDE5 [66]. It is believed that 8-position modification with the benzyl or phenylthio group mimics the cyclic ribose moiety of cAMP or cGMP. Although we have not tested the *cis* conformation of the styryl group, it has been shown in prior literature that the cis styryl group is a better inhibitor of PDE5 [28].

The use of different parasite strains, Tulahuen, Y, and CA-1 CL72, assisted in determining the efficiency of different levels, from sensitive, moderate resistance to complete resistance, of several drugs based on the literature [40–42]. To rule out the possibility of the impact of the PDE inhibitors at 100 nM of concentration on the host cell, cellular toxicity conditions, along with the survival of the cells, were determined by direct microscopic observation of the host cells (data not shown). Further, a more sensitive assay, CCK-8, was performed against the compounds to determine the cytotoxicity of the molecules on the host cells. None of the xanthine analogs showed any cytotoxicity to the mammalian cells, while one concentration indicated that these compounds were not cytotoxic at 100 nM; future studies will determine the toxicity of the lead molecules at various concentrations, and the IC_{50} value will be determined and compared to the IC_{50} value against parasites. The selectivity index ratio clearly shows the selectivity of these molecules toward *T. cruzi* compared to RHM cells (Table S1). Thus, these molecules are less toxic to host RHM cells, providing the desirable therapeutic window for the treatment. The predictive ADMET scores obtained using admetSAR 2.0 shows that these molecules have drug-like properties and fall within the desired properties, with the exception of water solubility.

We used amastigotes to test the most potent compound identified in the present screening. Amastigotes are a great model to investigate the biological role of specific gene recombination studies. There is a potential need to investigate the mode of action of new drug candidates by directly targeting the amastigote itself. Several drug screening studies have been conducted by targeting the axenic amastigotes in *Leishmania* [67–70], and many of the studies have shown that the inhibitory compounds identified by cellular and axenic amastigotes assays do not perfectly overlap [71,72] because of physiological differences in the proteomes and transcriptomes of *Leishmania* amastigotes [73,74]. Similar physiological differences between the two forms of amastigotes of *T. cruzi* have also been reported. For example, axenic amastigotes are completely resistant to complement-mediated lysis compared to intracellular amastigotes, where 100% of intracellular amastigotes were lysed in fresh serum. In terms of infection efficiency, experiments using axenic-cultured amastigotes were more infectious compared to the intracellularly derived amastigotes of *T. cruzi* [75]. Very limited studies have investigated therapeutic strategies against the *T. cruzi* axenic amastigotes [51]. Our study shows successful inhibition of the cellular and axenic amastigotes using the xanthine analogs and the non-toxicity of xanthine analogs in mammalian cells.

GVK14 showed remarkable inhibition of amastigote growth compared to the control drugs. Lower EC_{50} values were observed when GVK14 was used against all three strains, which opposes the notion of any potential difference related to parasite strain. Moreover, similar potency was observed against amastigotes when GVK14 was used axenically. This

disproves the possibility that these PDE inhibitors act directly on the amastigotes by impacting the host cell metabolism.

Since the PDEs identified in *T. cruzi* have a high affinity to cAMP, we have determined the cAMP levels that could provide evidence that IBMX analogs inhibit PDEs. We have also found that treatment with IBMX analogs increases cAMP levels significantly in many of these analogs.

The current study uses IBMX analogs that were originally designed to inhibit mammalian PDE5 and PDE1. The compounds used in this study do not inhibit mammalian cAMP PDEs but elevate the levels of cAMP in *T. cruzi*-infected myoblasts. Our study provides evidence that these molecules suppress *T. cruzi* infection in cardiac myoblasts with the most active compound, GVK14. GVK14 was also shown to suppress all three strains of *T. cruzi* with high potency. In terms of GVK14 drug-likeness, we also predicted its ADMET, along with all the other IBMX analogs we utilized in the experiment. Similar to IBMX, GVK14 is predicted to have human oral bioavailability and human intestinal bioavailability but with no hepatotoxicity or nephrotoxicity (Table S2). The majority of the xanthine analogs show slight acute oral toxicity and are non-carcinogenic. Based on the predictive model, the majority of the xanthine analogs are not only efficient against *T.cruzi* but can also be safe at therapeutic doses. One important observation that was made in this study was that the PDEs in *T. cruzi* have a tolerance for the electron-withdrawing groups on the benzyl moiety. This is important because such groups are not tolerated by mammalian PDEs. Thus, we can design molecules that are specific to *T. cruzi* PDEs. We plan to synthesize xanthine analogs with electron-withdrawing groups such as nitro, carboxy, carboxy esters, cyano, and keto groups on benzyl substitution at the 8-position to suppress their effect on host cell PDEs. We will also optimize the groups at the 1- and 3-positions with various alkyl or aryl groups to achieve parasite selective inhibitors. Based on our findings, we will also generate analogs of zaprinast with similar substitutions. The compounds will be tested on both parasite and host cell PDEs to determine their selectivity and sensitivity towards the particular PDE of *T. cruzi*. Further, *T. cruzi* genome analysis is required to predict the cAMP-binding proteins and their function. Thus, future modifications of IBMX will delineate the optimal substitutions required for *T. cruzi* inhibition in vivo. In addition, we will plan to study the efficacy of xanthine analog treatment on the various stages of Chagas diseases, namely, acute, intermediate, and chronic stages.

Supplementary Materials: The following are available online at https://www.mdpi.com/article/10.3390/microbiolres13040052/s1, Table S1: Selectivity Index (SI) of the Xanthine Analogues against various strains; Table S2: ADMET properties of Xanthine Analogues.

Institutional Review Board Statement: Not applicable.

Informed Consent Statement: Not applicable.

Data Availability Statement: All the experimental data is available in the corresponding author's and collaborators' laboratories.

References

1. Chagas WHO. Available online: https://www.who.int/data/gho/data/themes/neglected-tropical-diseases (accessed on 11 July 2022).
2. mondiale de la Santé, O.; World Health Organization. Chagas disease in Latin America: An epidemiological update based on 2010 estimates. *Wkly. Epidemiol. Rec.* **2015**, *90*, 33–43.
3. Prata, A. Clinical and epidemiological aspects of Chagas disease. *Lancet Infect. Dis.* **2001**, *1*, 92–100. [CrossRef]
4. Fernandes, M.C.; Flannery, A.R.; Andrews, N.; Mortara, R.A. Extracellular amastigotes of Trypanosoma cruzi are potent inducers of phagocytosis in mammalian cells. *Cell Microbiol.* **2013**, *15*, 977–991. [CrossRef] [PubMed]
5. Dias, J.C. The indeterminate form of human chronic Chagas' disease A clinical epidemiological review. *Rev. Soc. Bras. Med. Trop.* **1989**, *22*, 147–156. [CrossRef] [PubMed]
6. Bustamante, J.M.; Rivarola, H.W.; Fernandez, A.R.; Enders, J.E.; Fretes, R.; Palma, J.A.; Paglini-Oliva, P.A. Indeterminate Chagas' disease: Trypanosoma cruzi strain and re-infection are factors involved in the progression of cardiopathy. *Clin. Sci. (Lond)* **2003**, *104*, 415–420. [CrossRef]
7. Tanowitz, H.B.; Machado, F.S.; Jelicks, L.A.; Shirani, J.; de Carvalho, A.C.; Spray, D.C.; Factor, S.M.; Kirchhoff, L.V.; Weiss, L.M. Perspectives on Trypanosoma cruzi-induced heart disease (Chagas disease). *Prog. Cardiovasc. Dis.* **2009**, *51*, 524–539. [CrossRef]
8. Córdova, E.; Maiolo, E.; Corti, M.; Orduña, T. Neurological manifestations of Chagas' disease. *Neurol. Res.* **2010**, *32*, 238–244. [CrossRef]
9. Rodriques Coura, J.; de Castro, S.L. A critical review on Chagas disease chemotherapy. *Mem Inst. Oswaldo Cruz.* **2002**, *97*, 3–24. [CrossRef]
10. Bermudez, J.; Davies, C.; Simonazzi, A.; Real, J.P.; Palma, S. Current drug therapy and pharmaceutical challenges for Chagas disease. *Acta Trop.* **2016**, *156*, 1–16. [CrossRef]
11. Villalta, F.; Rachakonda, G. Advances in preclinical approaches to Chagas disease drug discovery. *Expert Opin. Drug Discov.* **2019**, *14*, 1161–1174. [CrossRef]
12. Sales Junior, P.A.; Molina, I.; Fonseca Murta, S.M.; Sanchez-Montalva, A.; Salvador, F.; Correa-Oliveira, R.; Carneiro, C.M. Experimental and Clinical Treatment of Chagas Disease: A Review. *Am. J. Trop Med. Hyg.* **2017**, *97*, 1289–1303. [CrossRef] [PubMed]
13. Martinez, S.J.; Romano, P.S.; Engman, D.M. Precision Health for Chagas Disease: Integrating Parasite and Host Factors to Predict Outcome of Infection and Response to Therapy. *Front. Cell Infect. Microbiol.* **2020**, *10*, 210. [CrossRef] [PubMed]
14. Pastan, I.H.; Johnson, G.S.; Anderson, W.B. Role of cyclic nucleotides in growth control. *Annu. Rev. Biochem.* **1975**, *44*, 491–522. [CrossRef] [PubMed]
15. Biswas, A.; Bhattacharya, A.; Das, P.K. Role of cAMP Signaling in the Survival and Infectivity of the Protozoan Parasite, *Leishmania donovani. Mol. Biol. Int.* **2011**, *2011*, 782971. [CrossRef]
16. Keravis, T.; Lugnier, C. Cyclic nucleotide phosphodiesterase (PDE) isozymes as targets of the intracellular signalling network: Benefits of PDE inhibitors in various diseases and perspectives for future therapeutic developments. *Br. J. Pharmacol.* **2012**, *165*, 1288–1305. [CrossRef] [PubMed]
17. Seebeck, T.; Schaub, R.; Johner, A. cAMP signalling in the kinetoplastid protozoa. *Curr. Mol. Med.* **2004**, *4*, 585–599. [CrossRef]
18. Alonso, G.D.; Schoijet, A.C.; Torres, H.N.; Flawia, M.M. TcPDE4, a novel membrane-associated cAMP-specific phosphodiesterase from Trypanosoma cruzi. *Mol. Biochem. Parasitol.* **2006**, *145*, 40–49. [CrossRef]
19. Diaz-Benjumea, R.; Laxman, S.; Hinds, T.R.; Beavo, J.A.; Rascon, A. Characterization of a novel cAMP-binding, cAMP-specific cyclic nucleotide phosphodiesterase (TcrPDEB1) from Trypanosoma cruzi. *Biochem. J.* **2006**, *399*, 305–314. [CrossRef]
20. Laxman, S.; Beavo, J.A. Cyclic nucleotide signaling mechanisms in trypanosomes: Possible targets for therapeutic agents. *Mol. Interv.* **2007**, *7*, 203–215. [CrossRef]
21. Oberholzer, M.; Marti, G.; Baresic, M.; Kunz, S.; Hemphill, A.; Seebeck, T. The Trypanosoma brucei cAMP phosphodiesterases TbrPDEB1 and TbrPDEB2: Flagellar enzymes that are essential for parasite virulence. *FASEB J.* **2007**, *21*, 720–731. [CrossRef]
22. Schoijet, A.C.; Miranda, K.; Medeiros, L.C.; de Souza, W.; Flawia, M.M.; Torres, H.N.; Pignataro, O.P.; Docampo, R.; Alonso, G.D. Defining the role of a FYVE domain in the localization and activity of a cAMP phosphodiesterase implicated in osmoregulation in Trypanosoma cruzi. *Mol. Microbiol.* **2011**, *79*, 50–62. [CrossRef] [PubMed]
23. Wang, H.; Kunz, S.; Chen, G.; Seebeck, T.; Wan, Y.; Robinson, H.; Martinelli, S.; Ke, H. Biological and structural characterization of Trypanosoma cruzi phosphodiesterase C and Implications for design of parasite selective inhibitors. *J. Biol. Chem.* **2012**, *287*, 11788–11797. [CrossRef]
24. Tagoe, D.N.; Kalejaiye, T.D.; de Koning, H.P. The ever unfolding story of cAMP signaling in trypanosomatids: Vive la difference! *Front. Pharmacol.* **2015**, *6*, 185. [CrossRef] [PubMed]

25. de Araujo, J.S.; Garcia-Rubia, A.; Sebastian-Perez, V.; Kalejaiye, T.D.; Bernardino da Silva, P.; Fonseca-Berzal, C.R.; Maes, L.; De Koning, H.P.; Soeiro, M.N.C.; Gil, C. Imidazole Derivatives as Promising Agents for the Treatment of Chagas Disease. *Antimicrob. Agents Chemother.* **2019**, *63*, e02156-18. [CrossRef]

26. Li, H.; Zuo, J.; Tang, W. Phosphodiesterase-4 Inhibitors for the Treatment of Inflammatory Diseases. *Front. Pharmacol.* **2018**, *9*, 1048. [CrossRef]

27. Spina, D.; Landells, L.J.; Page, C.P. The role of phosphodiesterase enzymes in allergy and asthma. *Adv. Pharmacol.* **1998**, *44*, 33–89. [CrossRef] [PubMed]

28. Sekhar, K.R.; Grondin, P.; Francis, S.H.; Corbin, J.D. *Design and Synthesis of Xanthines and Cyclic GMP Analogues as Potent Inhibitors of PDE5*; Academic Press: Cambridge, MA, USA, 1996.

29. Azevedo, M.F.; Faucz, F.R.; Bimpaki, E.; Horvath, A.; Levy, I.; de Alexandre, R.B.; Ahmad, F.; Manganiello, V.; Stratakis, C.A. Clinical and molecular genetics of the phosphodiesterases (PDEs). *Endocr. Rev.* **2014**, *35*, 195–233. [CrossRef]

30. Wang, Y.; Chackalamannil, S.; Hu, Z.; Boyle, C.D.; Lankin, C.M.; Xia, Y.; Xu, R.; Asberom, T.; Pissarnitski, D.; Stamford, A.W.; et al. Design and synthesis of xanthine analogues as potent and selective PDE5 inhibitors. *Bioorg. Med. Chem. Lett.* **2002**, *12*, 3149–3152. [CrossRef]

31. Woodring, J.L.; Pollastri, M.P. Inhibitors of protozoan phosphodiesterases as potential therapeutic approaches for tropical diseases. *Phosphodiesterases Inhib.* **2014**, *12*, 191–210.

32. Xie, J.; Wu, W.; Li, S.; Hu, Y.; Hu, M.; Li, J.; Yang, Y.; Huang, T.; Zheng, K.; Wang, Y.; et al. Clinical characteristics and outcomes of critically ill patients with novel coronavirus infectious disease (COVID-19) in China: A retrospective multicenter study. *Intensive Care Med.* **2020**, *46*, 1863–1872. [CrossRef]

33. King-Keller, S.; Li, M.; Smith, A.; Zheng, S.; Kaur, G.; Yang, X.; Wang, B.; Docampo, R. Chemical validation of phosphodiesterase C as a chemotherapeutic target in Trypanosoma cruzi, the etiological agent of Chagas' disease. *Antimicrob. Agents Chemother.* **2010**, *54*, 3738–3745. [CrossRef] [PubMed]

34. Zingales, B.; Andrade, S.G.; Briones, M.R.; Campbell, D.A.; Chiari, E.; Fernandes, O.; Guhl, F.; Lages-Silva, E.; Macedo, A.M.; Machado, C.R.; et al. A new consensus for Trypanosoma cruzi intraspecific nomenclature: Second revision meeting recommends TcI to TcVI. *Mem. Inst. Oswaldo Cruz.* **2009**, *104*, 1051–1054. [CrossRef] [PubMed]

35. Zingales, B.; Miles, M.A.; Campbell, D.A.; Tibayrenc, M.; Macedo, A.M.; Teixeira, M.M.; Schijman, A.G.; Llewellyn, M.S.; Lages-Silva, E.; Machado, C.R.; et al. The revised Trypanosoma cruzi subspecific nomenclature: Rationale, epidemiological relevance and research applications. *Infect. Genet. Evol* **2012**, *12*, 240–253. [CrossRef] [PubMed]

36. Marcili, A.; Lima, L.; Cavazzana, M.; Junqueira, A.C.; Veludo, H.H.; Maia Da Silva, F.; Campaner, M.; Paiva, F.; Nunes, V.L.; Teixeira, M.M. A new genotype of Trypanosoma cruzi associated with bats evidenced by phylogenetic analyses using SSU rDNA, cytochrome b and Histone H2B genes and genotyping based on ITS1 rDNA. *Parasitology* **2009**, *136*, 641–655. [CrossRef]

37. Hall, B.S.; Wilkinson, S.R. Activation of benznidazole by trypanosomal type I nitroreductases results in glyoxal formation. *Antimicrob. Agents Chemother.* **2012**, *56*, 115–123. [CrossRef]

38. Guedes, P.M.; Urbina, J.A.; de Lana, M.; Afonso, L.C.; Veloso, V.M.; Tafuri, W.L.; Machado-Coelho, G.L.; Chiari, E.; Bahia, M.T. Activity of the new triazole derivative albaconazole against Trypanosoma (Schizotrypanum) cruzi in dog hosts. *Antimicrob. Agents Chemother.* **2004**, *48*, 4286–4292. [CrossRef]

39. Stothard, J.; Frame, I.; Miles, M. Genetic diversity and genetic exchange in Trypanosoma cruzi: Dual drug-resistant "progeny" from episomal transformants. *Mem. Inst. Oswaldo Cruz.* **1999**, *94* (Suppl. S1), 189–193. [CrossRef]

40. Grosso, N.L.; Bua, J.; Perrone, A.E.; Gonzalez, M.N.; Bustos, P.L.; Postan, M.; Fichera, L.E. Trypanosoma cruzi: Biological characterization of a isolate from an endemic area and its susceptibility to conventional drugs. *Exp. Parasitol.* **2010**, *126*, 239–244. [CrossRef]

41. Lima, M.F.; Villalta, F. Trypanosoma cruzi trypomastigote clones differentially express a parasite cell adhesion molecule. *Mol. Biochem. Parasitol.* **1989**, *33*, 159–170. [CrossRef]

42. Luna, K.P.; Hernandez, I.P.; Rueda, C.M.; Zorro, M.M.; Croft, S.L.; Escobar, P. In vitro susceptibility of Trypanosoma cruzi strains from Santander, Colombia, to hexadecylphosphocholine (miltefosine), nifurtimox and benznidazole. *Biomedica* **2009**, *29*, 448–455.

43. Nozaki, T.; Engel, J.C.; Dvorak, J.A. Cellular and molecular biological analyses of nifurtimox resistance in Trypanosoma cruzi. *Am. J. Trop. Med. Hyg.* **1996**, *55*, 111–117. [CrossRef]

44. Perez, C.J.; Lymbery, A.J.; Thompson, R.C. Chagas disease: The challenge of polyparasitism? *Trends Parasitol.* **2014**, *30*, 176–182. [CrossRef] [PubMed]

45. Gonçalves, C.S.; Ávila, A.R.; de Souza, W.; Motta, M.C.M.; Cavalcanti, D.P. Revisiting the Trypanosoma cruzi metacyclogenesis: Morphological and ultrastructural analyses during cell differentiation. *Parasites Vectors* **2018**, *11*, 83. [CrossRef] [PubMed]

46. Johnson, C.A.; Kleshchenko, Y.Y.; Ikejiani, A.O.; Udoko, A.N.; Cardenas, T.C.; Pratap, S.; Duquette, M.A.; Lima, M.F.; Lawler, J.; Villalta, F.; et al. Thrombospondin-1 interacts with Trypanosoma cruzi surface calreticulin to enhance cellular infection. *PLoS ONE* **2012**, *7*, e40614. [CrossRef] [PubMed]

47. Lepesheva, G.I.; Hargrove, T.Y.; Anderson, S.; Kleshchenko, Y.; Furtak, V.; Wawrzak, Z.; Villalta, F.; Waterman, M.R. Structural insights into inhibition of sterol 14alpha-demethylase in the human pathogen Trypanosoma cruzi. *J. Biol. Chem.* **2010**, *285*, 25582–25590. [CrossRef] [PubMed]

48. Villalta, F.; Dobish, M.C.; Nde, P.N.; Kleshchenko, Y.Y.; Hargrove, T.Y.; Johnson, C.A.; Waterman, M.R.; Johnston, J.N.; Lepesheva, G.I. VNI cures acute and chronic experimental Chagas disease. *J. Infect. Dis.* **2013**, *208*, 504–511. [CrossRef]

49. Lepesheva, G.I.; Hargrove, T.Y.; Rachakonda, G.; Wawrzak, Z.; Pomel, S.; Cojean, S.; Nde, P.N.; Nes, W.D.; Locuson, C.W.; Calcutt, M.W.; et al. VFV as a New Effective CYP51 Structure-Derived Drug Candidate for Chagas Disease and Visceral Leishmaniasis. *J. Infect. Dis.* **2015**, *212*, 1439–1448. [CrossRef]

50. Villalta, F.; Kierszenbaum, F. Growth of isolated amastigotes of Trypanosoma cruzi in cell-free medium. *J. Protozool.* **1982**, *29*, 570–576. [CrossRef]

51. Pate, P.G.; Wolfson, J.S.; McHugh, G.L.; Pan, S.C.; Swartz, M.N. Novobiocin antagonism of amastigotes of Trypanosoma cruzi growing in cell-free medium. *Antimicrob. Agents Chemother.* **1986**, *29*, 426–431. [CrossRef]

52. Udoko, A.N.; Johnson, C.A.; Dykan, A.; Rachakonda, G.; Villalta, F.; Mandape, S.N.; Lima, M.F.; Pratap, S.; Nde, P.N. Early Regulation of Profibrotic Genes in Primary Human Cardiac Myocytes by Trypanosoma cruzi. *PLoS Negl. Trop Dis.* **2016**, *10*, e0003747. [CrossRef]

53. Hoekstra, W.J.; Hargrove, T.Y.; Wawrzak, Z.; da Gama Jaen Batista, D.; da Silva, C.F.; Nefertiti, A.S.; Rachakonda, G.; Schotzinger, R.J.; Villalta, F.; Soeiro Mde, N.; et al. Clinical Candidate VT-1161's Antiparasitic Effect In Vitro, Activity in a Murine Model of Chagas Disease, and Structural Characterization in Complex with the Target Enzyme CYP51 from Trypanosoma cruzi. *Antimicrob. Agents Chemother.* **2016**, *60*, 1058–1066. [CrossRef] [PubMed]

54. Vela, A.; Coral-Almeida, M.; Sereno, D.; Costales, J.A.; Barnabe, C.; Breniere, S.F. In vitro susceptibility of Trypanosoma cruzi discrete typing units (DTUs) to benznidazole: A systematic review and meta-analysis. *PLoS Negl. Trop Dis.* **2021**, *15*, e0009269. [CrossRef] [PubMed]

55. Yang, H.; Sun, L.; Wang, Z.; Li, W.; Liu, G.; Tang, Y. ADMETopt: A Web Server for ADMET Optimization in Drug Design via Scaffold Hopping. *J. Chem. Inf. Model.* **2018**, *58*, 2051–2056. [CrossRef] [PubMed]

56. Backman, T.W.; Cao, Y.; Girke, T. ChemMine tools: An online service for analyzing and clustering small molecules. *Nucleic Acids Res.* **2011**, *39*, W486–W491. [CrossRef] [PubMed]

57. Turko, I.V.; Ballard, S.A.; Francis, S.H.; Corbin, J.D. Inhibition of cyclic GMP-binding cyclic GMP-specific phosphodiesterase (Type 5) by sildenafil and related compounds. *Mol. Pharmacol.* **1999**, *56*, 124–130. [CrossRef]

58. Daugan, A.; Grondin, P.; Ruault, C.; Le Monnier de Gouville, A.C.; Coste, H.; Kirilovsky, J.; Hyafil, F.; Labaudiniere, R. The discovery of tadalafil: A novel and highly selective PDE5 inhibitor. 1: 5,6,11,11a-tetrahydro-1H-imidazo [1′,5′:1,6]pyrido[3,4-b]indole-1,3(2H)-dione analogues. *J. Med. Chem.* **2003**, *46*, 4525–4532. [CrossRef]

59. Broccatelli, F.; Carosati, E.; Neri, A.; Frosini, M.; Goracci, L.; Oprea, T.I.; Cruciani, G. A novel approach for predicting P-glycoprotein (ABCB1) inhibition using molecular interaction fields. *J. Med. Chem.* **2011**, *54*, 1740–1751. [CrossRef]

60. Da Mata, J.R.; Camargos, M.R.; Chiari, E.; Machado, C.R. Trypanosoma cruzi infection and the rat central nervous system: Proliferation of parasites in astrocytes and the brain reaction to parasitism. *Brain Res. Bull.* **2000**, *53*, 153–162. [CrossRef]

61. Williams, J.A.; Hyland, R.; Jones, B.C.; Smith, D.A.; Hurst, S.; Goosen, T.C.; Peterkin, V.; Koup, J.R.; Ball, S.E. Drug-drug interactions for UDP-glucuronosyltransferase substrates: A pharmacokinetic explanation for typically observed low exposure (AUCi/AUC) ratios. *Drug Metab. Dispos.* **2004**, *32*, 1201–1208. [CrossRef]

62. Kido, Y.; Matsson, P.; Giacomini, K.M. Profiling of a prescription drug library for potential renal drug-drug interactions mediated by the organic cation transporter 2. *J. Med. Chem.* **2011**, *54*, 4548–4558. [CrossRef]

63. Neitz, R.J.; Chen, S.; Supek, F.; Yeh, V.; Kellar, D.; Gut, J.; Bryant, C.; Gallardo-Godoy, A.; Molteni, V.; Roach, S.L.; et al. Lead identification to clinical candidate selection: Drugs for Chagas disease. *J. Biomol. Screen* **2015**, *20*, 101–111. [CrossRef] [PubMed]

64. Francis, S.H.; Sekhar, K.R.; Ke, H.; Corbin, J.D. Inhibition of cyclic nucleotide phosphodiesterases by methylxanthines and related compounds. *Handb. Exp. Pharmacol.* **2011**, *34*, 93–133. [CrossRef]

65. Choi, S.H.; Choi, D.H.; Song, K.S.; Shin, K.H.; Chun, B.G. Zaprinast, an inhibitor of cGMP-selective phosphodiesterases, enhances the secretion of TNF-alpha and IL-1beta and the expression of iNOS and MHC class II molecules in rat microglial cells. *J. Neurosci. Res.* **2002**, *67*, 411–421. [CrossRef]

66. Ahmed, W.S.; Geethakumari, A.M.; Biswas, K.H. Phosphodiesterase 5 (PDE5): Structure-function regulation and therapeutic applications of inhibitors. *Biomed. Pharmacother.* **2021**, *134*, 111128. [CrossRef] [PubMed]

67. Teixeira, M.C.; de Jesus Santos, R.; Sampaio, R.B.; Pontes-de-Carvalho, L.; dos-Santos, W.L. A simple and reproducible method to obtain large numbers of axenic amastigotes of different Leishmania species. *Parasitol. Res.* **2002**, *88*, 963–968. [CrossRef] [PubMed]

68. Shimony, O.; Jaffe, C.L. Rapid fluorescent assay for screening drugs on Leishmania amastigotes. *J. Microbiol. Methods* **2008**, *75*, 196–200. [CrossRef] [PubMed]

69. Nuhs, A.; De Rycker, M.; Manthri, S.; Comer, E.; Scherer, C.A.; Schreiber, S.L.; Ioset, J.R.; Gray, D.W. Development and Validation of a Novel Leishmania donovani Screening Cascade for High-Throughput Screening Using a Novel Axenic Assay with High Predictivity of Leishmanicidal Intracellular Activity. *PLoS Negl. Trop. Dis.* **2015**, *9*, e0004094. [CrossRef]

70. Bhaskar, R.; Gangwar, S.; Goyal, N. Development of luciferase expressing Leishmania donovani axenic amastigotes as primary model for in vitro screening of antileishmanial compounds. *Curr. Microbiol.* **2012**, *65*, 696–700. [CrossRef]

71. De Rycker, M.; Hallyburton, I.; Thomas, J.; Campbell, L.; Wyllie, S.; Joshi, D.; Cameron, S.; Gilbert, I.H.; Wyatt, P.G.; Frearson, J.A.; et al. Comparison of a high-throughput high-content intracellular Leishmania donovani assay with an axenic amastigote assay. *Antimicrob. Agents Chemother.* **2013**, *57*, 2913–2922. [CrossRef]

72. Debrabant, A.; Joshi, M.B.; Pimenta, P.F.; Dwyer, D.M. Generation of Leishmania donovani axenic amastigotes: Their growth and biological characteristics. *Int. J. Parasitol.* **2004**, *34*, 205–217. [CrossRef]

73. Pescher, P.; Blisnick, T.; Bastin, P.; Spath, G.F. Quantitative proteome profiling informs on phenotypic traits that adapt Leishmania donovani for axenic and intracellular proliferation. *Cell Microbiol.* **2011**, *13*, 978–991. [CrossRef] [PubMed]
74. Rochette, A.; Raymond, F.; Corbeil, J.; Ouellette, M.; Papadopoulou, B. Whole-genome comparative RNA expression profiling of axenic and intracellular amastigote forms of Leishmania infantum. *Mol. Biochem. Parasitol.* **2009**, *165*, 32–47. [CrossRef] [PubMed]
75. Fernandes, A.B.; Mortara, R.A. Invasion of MDCK epithelial cells with altered expression of Rho GTPases by Trypanosoma cruzi amastigotes and metacyclic trypomastigotes of strains from the two major phylogenetic lineages. *Microbes Infect.* **2004**, *6*, 460–467. [CrossRef] [PubMed]